



Non-linear Axial Vibrations of Composite Drill Strings Considering Interaction of Roller Cone Bit and Polycrystalline Diamond Compact Bit with Rock

M. Mohammadzadeh^a, M. Arbabtafti^{*a}, M. Shahgholi^a, J. Yang^b

^a Faculty of Mechanical Engineering, Shahid Rajaei Teacher Training University, Tehran, Iran

^b Faculty of Engineering and Applied Science, Memorial University of Newfoundland, St. John's, NL, Canada

PAPER INFO

Paper history:

Received 10 November 2020

Received in revised form 18 December 2020

Accepted 03 February 2021

Keywords:

Bit-rock Interaction

Composite Drill Strings

Finite Element

Non-linear Axial Vibrations

ABSTRACT

Due to the world increasing energy demands, optimizing the drilling system parameters such as the weight on bit (WOB), and the structure of drill string and bit, also vibrations and dynamic behavior of drill strings are of significant interest to researchers and energy industries. Specially, to overcome limitations of drilling operations in oil and gas industry, composite drill strings as high-tech devices are under development. In this research, the fully coupled non-linear axial vibrations of composite drill strings due to the interaction of two common bits namely; Roller Cone (RC) and Polycrystalline Diamond Compact (PDC) with rock, considering the major non-linear terms, the drill string-wellbore contact, the different weight on bit (WOB) and the different composite configurations using the finite element method (FEM) and the Lagrangian approach were studied. This study proved that the different configurations of composite drill strings showed specific dynamic behavior at different conditions. Therefore, composite drill string can be designed for particular purposes. Also, the results imply the remarkable effects of weight on bit (WOB) and type of bits on the axial vibrations of composite drill strings.

doi: 10.5829/ije.2021.34.04a.28

1. INTRODUCTION

A drill string is an ultra-slender rotor, which is suspended by a hoisting system on the surface, to connect the rotary drive system at the top to the bit at the bottom to dig through the rock. The drill string is put lower through the well to generate the compressional load applied on the bit F_{bit} , which is generally equal to the value of weight on bit (WOB). The upper and lower fragments of the drill string are the drill pipes and drill collars, respectively (see Figure 1).

The basic experimental and analytical analysis of vibrations of drill strings started in past decades [1-3]. Yigit and Christoforou [4] studied the coupled axial and transverse vibrations of oilwell drillstrings. Optimizing the drilling parameters such as weight on bit, rate of penetration (ROP) and structure of drill string and bit

are of great interest to researchers and energy industries, academically and practically [5-8]. The effects of downhole assembly and polycrystalline diamond compact (PDC) bit geometry on stability of drillstrings were studied by Elsayed et al. [9]. Jansen [10] analyzed the dynamic behavior of drill string considering the drilling fluid and drill string-wellbore contact. Jogi et al. [11] presented four programs to analyze vibrations. Spanos et al. [12] studied the drill string-wellbore contact using a nonlinear finite element dynamic model. Khulief and Al-Naser [13] analyzed dynamic of a finite element model of drill string. The system responses with the reduced-order and full-order models were compared. Ghasemloonia et al. [14] studied the coupled non-linear axial-transverse vibration of a drill string using the Bypassing PDE's method with the expanded Galerkin's method. Nowadays, the study on optimization of materials to improve their role in practical aspects are increasing [15-17]. In recent years, the use of new torsion shafts [18,19] and composite

*Corresponding Author Institutional Email: Arbabtafti@sru.ac.ir (M. Arbabtafti)

rotors [20, 21] is expanding. Specially, to overcome limitations of drilling operations in oil and gas industry, composite drill strings as high-tech devices are under development.

The composite drill strings can be designed to meet specific requirements for specific applications, e.g. flexible enough to resist bending fatigue, but strong enough to carry high tensional and torsional loads, particularly in the ultra-deep directional drilling or the short radius directional drilling [20-22].

Mohammadzadeh et al. [22] furnished a basic fully coupled non-linear model of composite drill strings for the further development of a more comprehensive model. The approach presented on that work[22] has been adapted in recent study and has been extended to accommodate the important case of non-linear axial vibrations considering bit (RC/PDC)-rock interaction.

This research has aimed to study the fully coupled non-linear axial vibrations of vertical composite drill strings due to the interaction of two common bits namely; Roller-Cone (RC) bits and Polycrystalline Diamond Compact (PDC) with rock, considering the drill string-wellbore contact, the different weight on bit (WOB) and the different composite configurations. Also, the gyroscopic effect, and especially the geometric stiffening effect, the axial-torsional-lateral coupling of vibrations and the major non-linear terms have been taken into account. The full-order non-linear equations of the whole length of drill string including

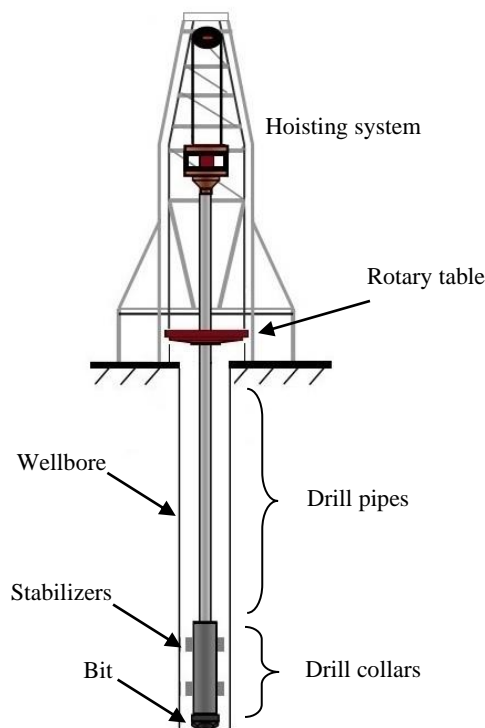


Figure 1. The drilling system

drill pipes and drill collars have been derived by the finite element method and the Lagrangian approach.

2. PROBLEM FORMULATION

The laminated composite drill string consists of the winded orthotropic layers.

2. 1. Finite Element Discretization Using a number of two-node elements with six degrees of freedom per node, the element displacement vector $\{e\}$ can be defined by Equation (1):

$$\{e\}_{12 \times 1} = [u_1 \ v_1 \ w_1 \ \theta_{x1} \ \theta_{y1} \ \theta_{z1} \ u_2 \ v_2 \ w_2 \ \theta_{x2} \ \theta_{y2} \ \theta_{z2}]^T \tag{1}$$

Figure 2 shows the translational displacements u, v, w , the torsional displacements θ_x , and the rotational displacements θ_y and θ_z in their directions. The nodal displacement functions can be expressed below:

$$u_e(x,t) = N_u(x) e(t) \quad \theta_{xe}(x,t) = N_{\theta_x}(x) e(t) \tag{2}$$

$$v_e(x,t) = N_v(x) e(t) \quad \theta_{ye}(x,t) = N_{\theta_y}(x) e(t)$$

$$w_e(x,t) = N_w(x) e(t) \quad \theta_{ze}(x,t) = N_{\theta_z}(x) e(t)$$

where N is the shape function based on Timoshenko beam theory [23-25].

2. 1. Kinetic Energy of the Composite Drill String

The kinetic energy of an element can be written as follows:

$$T = \frac{1}{2} \int_0^{L_e} \{ m \mathbf{V}^{tr} \mathbf{V} + \boldsymbol{\omega}^{tr} [\mathbf{I}] \boldsymbol{\omega} \} dx \tag{3}$$

where m is the mass per unit length, \mathbf{V} is translation velocity vector of the cross section, $\boldsymbol{\omega}$ is angular

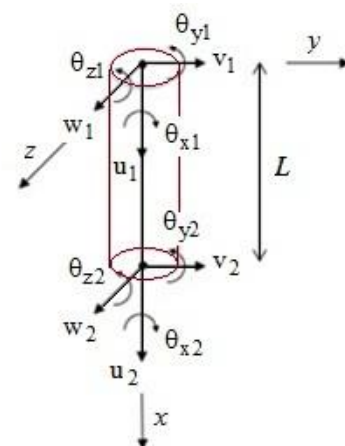


Figure 2. Degrees of freedom of an element

velocity vector in the fixed reference system and [I] is the matrix of mass moment of inertia stated as follows:

$$m = \frac{\pi}{4} \sum_{k=1}^n \rho_k (D_{ok}^2 - D_{ik}^2), \quad \mathbf{v} = \begin{pmatrix} \frac{\partial u}{\partial t} & \frac{\partial v}{\partial t} & \frac{\partial w}{\partial t} \end{pmatrix}^{tr}$$

$$\boldsymbol{\omega} = (\omega_x \quad \omega_y \quad \omega_z)^{tr}, \quad [I] = \text{Diag} [I_P \quad I_D \quad I_D]$$

Where

$$\omega_x = \left(\frac{\partial \Phi}{\partial t} + \frac{\partial \theta_x}{\partial t} \right) - \frac{\partial \theta_z}{\partial t} \theta_y \tag{4}$$

$$\omega_y = \frac{\partial \theta_y}{\partial t} \cos(\Phi + \theta_x) - \frac{\partial \theta_z}{\partial t} \sin(\Phi + \theta_x)$$

$$\omega_z = \frac{\partial \theta_y}{\partial t} \sin(\Phi + \theta_x) + \frac{\partial \theta_z}{\partial t} \cos(\Phi + \theta_x)$$

That I_P and I_D are the polar and diametrical mass moment of inertia. After some algebraic manipulations, the total kinetic energy of an element can be written as follows:

$$T = \frac{1}{2} \int_0^{L_e} \left\{ \frac{\pi}{4} \sum_{k=1}^n \rho_k (D_{ok}^2 - D_{ik}^2) \left(\frac{\partial u}{\partial t} \right)^2 + \frac{\pi}{4} \sum_{k=1}^n \rho_k (D_{ok}^2 - D_{ik}^2) \left(\frac{\partial v}{\partial t} \right)^2 \right. \\ + \frac{\pi}{4} \sum_{k=1}^n \rho_k (D_{ok}^2 - D_{ik}^2) \left(\frac{\partial w}{\partial t} \right)^2 + \frac{\pi}{32} \sum_{k=1}^n \rho_k (D_{ok}^4 - D_{ik}^4) \left(\frac{\partial(\Phi + \theta_x)}{\partial t} \right)^2 \\ + \frac{\pi}{64} \sum_{k=1}^n \rho_k (D_{ok}^4 - D_{ik}^4) \left(\frac{\partial \theta_y}{\partial t} \right)^2 + \frac{\pi}{64} \sum_{k=1}^n \rho_k (D_{ok}^4 - D_{ik}^4) \left(\frac{\partial \theta_z}{\partial t} \right)^2 \\ \left. - \frac{\pi}{32} \sum_{k=1}^n \rho_k (D_{ok}^4 - D_{ik}^4) \left[2 \left(\frac{\partial(\Phi + \theta_x)}{\partial t} \right) \left(\frac{\partial \theta_z}{\partial t} \right) \theta_y - \left(\frac{\partial \theta_z}{\partial t} \right)^2 \theta_y^2 \right] \right\} dx \tag{5}$$

That accounts for the translational inertia, the torsional inertia, the rotational inertia, and the coupling term comprise the non-linear terms and the gyroscopic moments. Also, n is the number of the layers, ρ_k is the material density of the k -th layer. As shown in Figure 3, D_{ok} and D_{ik} are the external and internal diameter of the k -th layer, respectively.

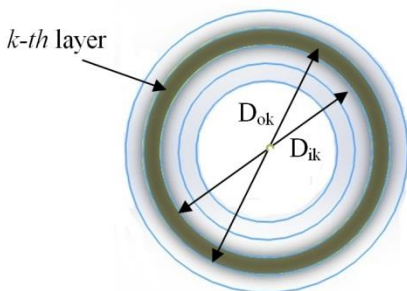


Figure 3. The external and internal diameter of the k -th layer

2. 2. Strain Energy of the Composite Drill String

The generalized Hooke’s law for fiber-reinforced composite materials in the cylindrical coordinate system can be expressed as follows:

$$\{\sigma\}_{x,\theta,r} = [\bar{C}]\{\varepsilon\}_{x,\theta,r} \tag{6}$$

Where $\{\sigma\}$ and $\{\varepsilon\}$ are the stress and strain fields, and $[\bar{C}]$ is the transformed stiffness matrix of a layer [26].

The strain energy of an element in the cylindrical coordinate system is given below:

$$U = \frac{1}{2} \int_V \{ \sigma_{xx} \varepsilon_{xx} + \sigma_{rr} \varepsilon_{rr} + \sigma_{\theta\theta} \varepsilon_{\theta\theta} \\ + 2\tau_{xr} \varepsilon_{xr} + 2\tau_{x\theta} \varepsilon_{x\theta} + 2\tau_{r\theta} \varepsilon_{r\theta} \} dV \tag{7}$$

Since the length of drill string is very bigger than the lateral dimensions, therefore:

$$\sigma_{rr}, \sigma_{\theta\theta}, \tau_{r\theta} \cong 0 \quad \text{and} \quad \varepsilon_{rr}, \varepsilon_{\theta\theta}, \varepsilon_{r\theta} \cong 0, \text{ thus:}$$

$$U = \frac{1}{2} \int_0^{L_e} \left\{ \frac{\pi}{4} \sum_{k=1}^n \bar{C}_{11k} (D_{ok}^2 - D_{ik}^2) \left(\frac{\partial u}{\partial x} \right)^2 \right. \\ + k_s \frac{\pi}{32} \sum_{k=1}^n \bar{C}_{66k} (D_{ok}^4 - D_{ik}^4) \left(\frac{\partial \theta_x}{\partial x} \right)^2 \\ + \frac{\pi}{64} \sum_{k=1}^n \bar{C}_{11k} (D_{ok}^4 - D_{ik}^4) \left(\frac{\partial \theta_y}{\partial x} \right)^2 \\ + \left(\frac{\partial \theta_z}{\partial x} \right)^2 + k_s \left(\frac{\pi}{8} \sum_{k=1}^n \bar{C}_{55k} (D_{ok}^2 - D_{ik}^2) \right. \\ + \frac{\pi}{8} \sum_{k=1}^n \bar{C}_{66k} (D_{ok}^2 - D_{ik}^2) \left. \left(\frac{\partial v}{\partial x} - \theta_z \right)^2 + \left(\frac{\partial w}{\partial x} + \theta_y \right)^2 \right) \\ + \frac{\pi}{4} \sum_{k=1}^n \bar{C}_{11k} (D_{ok}^2 - D_{ik}^2) \left(\frac{\partial u}{\partial x} \right)^3 + \frac{\partial u}{\partial x} \left(\frac{\partial v}{\partial x} \right)^2 + \frac{\partial u}{\partial x} \left(\frac{\partial w}{\partial x} \right)^2 \\ + \frac{3\pi}{64} \sum_{k=1}^n \bar{C}_{11k} (D_{ok}^4 - D_{ik}^4) \left(\frac{\partial u}{\partial x} \left(\frac{\partial \theta_y}{\partial x} \right)^2 + \frac{\partial u}{\partial x} \left(\frac{\partial \theta_z}{\partial x} \right)^2 \right) \\ + k_s \frac{\pi}{12} \sum_{k=1}^n \bar{C}_{16k} (D_{ok}^3 - D_{ik}^3) \\ \left. \times \left(2 \frac{\partial \theta_x}{\partial x} \frac{\partial u}{\partial x} - \frac{\partial \theta_y}{\partial x} \left(\frac{\partial v}{\partial x} - \theta_z \right) - \frac{\partial \theta_z}{\partial x} \left(\frac{\partial w}{\partial x} + \theta_y \right) \right) \right\} dx \tag{8}$$

Which accounts for the axial, the torsional, the bending and the non-linear shearing deformations. The last three terms represent other major non-linear low-order terms. The lateral stiffness of drill strings varies when they are subjected to high axial loads, this phenomenon is called the geometric stiffening effect [22, 27], the strain energy due to geometric stiffening effect is denoted by U_{gs} :

$$\begin{aligned}
U_{gs} = & \frac{1}{2} \int_0^{L_e} \left[\frac{\pi}{4} \sum_{k=1}^n \bar{C}_{11k} (D_{ok}^2 - D_{ik}^2) \right. \\
& \times \left(\left(\frac{\partial u}{\partial x} \right)^3 + \left(\frac{\partial u}{\partial x} \right) \left(\frac{\partial v}{\partial x} \right)^2 + \left(\frac{\partial u}{\partial x} \right) \left(\frac{\partial w}{\partial x} \right)^2 \right) \\
& \left. + \frac{3\pi}{64} \sum_{k=1}^n \bar{C}_{11k} (D_{ok}^4 - D_{ik}^4) \left(\left(\frac{\partial u}{\partial x} \right) \left(\frac{\partial \theta_y}{\partial x} \right)^2 + \left(\frac{\partial u}{\partial x} \right) \left(\frac{\partial \theta_z}{\partial x} \right)^2 \right) \right] dx \quad (9)
\end{aligned}$$

where, the term $\frac{\pi}{4} \sum_{k=1}^n \bar{C}_{11k} (D_{ok}^2 - D_{ik}^2)$ is the net axial force

$F_A(x)$ [27], then:

$$\begin{aligned}
U_{gs} = & \frac{1}{2} \int_0^{L_e} \left[F_A(x) \left(\left(\frac{\partial u}{\partial x} \right)^3 + \left(\frac{\partial u}{\partial x} \right) \left(\frac{\partial v}{\partial x} \right)^2 + \left(\frac{\partial u}{\partial x} \right) \left(\frac{\partial w}{\partial x} \right)^2 \right) \right. \\
& \left. + \frac{3\pi}{64} \sum_{k=1}^n \bar{C}_{11k} (D_{ok}^4 - D_{ik}^4) \left(\left(\frac{\partial u}{\partial x} \right) \left(\frac{\partial \theta_y}{\partial x} \right)^2 + \left(\frac{\partial u}{\partial x} \right) \left(\frac{\partial \theta_z}{\partial x} \right)^2 \right) \right] dx \quad (10)
\end{aligned}$$

The net axial force $F_A(x)$ in a point is the resultant of $W(x)$ the downward drill string weight and F_{bit} the upward reaction force between the bit and the bottom of the well formation. The upper parts of the drill string operate under axial tension, while the upward reaction force causes the lower parts operate under axial compression. There is a neutral point in drill strings, in which $F_A(x)=0$. So, $F_A(x)$ and U_{gs} must be defined for compression and tension fields (Figure 4).

2. 3. Drill String-wellbore Contact The contact loads between the drill string and wellbore at each point can be modeled by F_n the concentrated forces along normal and F_t tangential directions and M_f the frictional concentrated torque, so:

$$F_n = \begin{cases} 0 & \text{for } (\gamma \leq g) \\ -k_c(\gamma - g) & \text{for } (\gamma > g) \end{cases}, \quad (11)$$

$$F_t = \mu F_n \text{sign} \left(\frac{\partial \Phi}{\partial t} \right), \quad \text{and} \quad M_f = 0.5 D_o F_t$$

Where $\gamma = \sqrt{v^2 + w^2}$, $g = 0.5(D_{ch} - D_o)$

γ is the radial displacement of the drill string, g is the gap between the surface of the drill string and the wellbore surface, k_c is the stiffness of contact to simulate normal force F_n as an elastic force, μ is the frictional coefficient, D_{ch} and is the wellbore diameter and D_o is the external diameter of drill string.

2. 4. Bit-rock Interaction The main process of drilling in oil and gas industries is the creation of borehole by a rock-cutting tool called a bit. Traditional bits consist of a steel body equipped with three rotating conical cylinder with steel teeth that crush the rock, Roller-Cone (RC) bits. Modern bits often consist of a steel body without rotating parts, covered with artificial

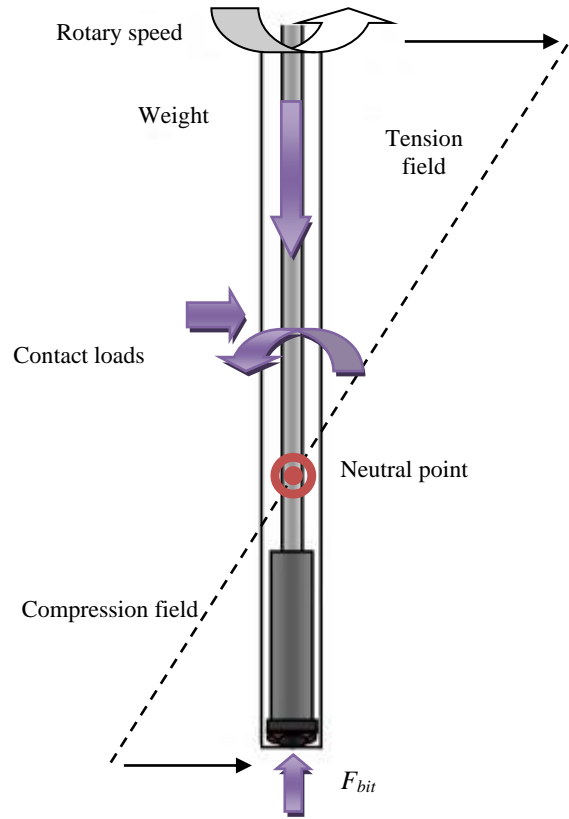


Figure 4. The general scheme of the loads

diamond cutters that shear the rock, Polycrystalline Diamond Compact (PDC) bits (Figures 5).

The frequency of contact force between PDC bit and rock is equal to the angular velocity of rotary table, while the frequency of contact force between RC bit and rock is three times the angular velocity of rotary table [9]. So, the two continuous forces, which are applied in the axial direction at the end of the bit, have been assumed to simulate the interaction of these bits and rock, respectively. The forces are expressed as follow:

$$F_{RC-bit} = WOB \sin(3\Omega t) \quad (12)$$

$$F_{PDC-bit} = WOB \sin(\Omega t)$$

2. 5. Dynamic Equation of Motion The dynamic equation of motion can be derived using the Lagrange's equation, which can be given below:

$$\frac{d}{dt} \left(\frac{\partial L}{\partial \dot{q}} \right) - \frac{\partial L}{\partial q} = Q \quad (13)$$

where $L = (T - U)$ is the Lagrangian function, q and Q are the vectors of generalized coordinates and



Figure 5 (a) RC bit



Figure 5 (b) PDC bit

generalized forces, respectively. The expressions of the component terms of Equation (1) have been integrated into computational scheme to obtain the results.

3. SIMULATION AND RESULTS ANALYSIS

The full-order non-linear dynamic equations of composite drill string were solved using a computational plan in MATLAB. The drill string was discretized into 240 elements to achieve results convergence. Table 1 shows the two 16-orthotropic-layer cases with different configurations to show major trends. Also, Table 2 displays the used data in simulation.

It is assumed that the lateral translations and the lateral rotations are zero at the top. The lateral translations at the bit are also zero. The vertical drill string at the top node is subjected to the constant

TABLE 1. The under investigation cases

Case	1	2
Configuration	$[\pm 75]_8$	$[\pm 15]_8$

TABLE 2. The used data in simulation

Drill string length = 1200 m	$E_1=141.343$ GPa
Drill pipes length = 1000 m	$E_2= E_3=9.563$ GPa
Drill pipes OD/ID = 0.1524/0.127 m	$G_{12}= G_{13}=4.55$ GPa
Drill collars length =200 m	$G_{23}=2.85$ Gpa
Drill collars OD/ID = 0.2324/0.1062 m	$\nu_{12}= \nu_{13}=0.28$
Wellbore diameter = 0.3524 m	$\nu_{23}=0.517$
Contact stiffness = 10e8 N/m	$\rho= 3930$ kg/m ³
Frictional coefficient = 5e-4	
Constant angular velocity = 6 Rad/s	
The first stabilizer location = 50 m above the bottom,	
The second stabilizer location = 150 m above the bottom	

angular velocity about the x-axis and then WOB is applied. The general scheme of loads has been displayed in Figure 4.

The WOB values have been assumed 10 and 30% of the drill collars weight. Figures 6-13 show the axial vibrations of end point of drill collar, which is located at 200 m above the bit.

Figures 6 and 7 show the axial deflections, when WOB is 10% of the drill collars weight for PDC bits in cases 1 and 2, respectively.

The axial deflections, when WOB is 10% of the drill collars weight for RC bits in cases 1 and 2 are displayed in Figures 8 and 9, respectively.

When the ply angle decreases, due to increase of axial stiffness, firstly; the maximum amplitudes of responses decrease; secondly, the capability of drill string to transmit the axial vibrations increases, and the drill string become more sensitive to excitations, so the drill string experience the denser axial vibrations at a point above the bit, as shown in Figures 6 and 7.

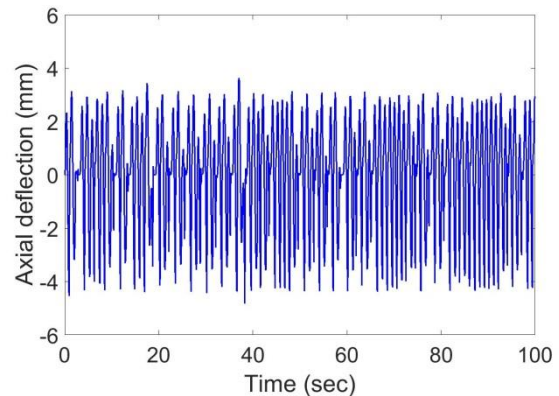


Figure 6. Axial deflection at 200 m above the bit, WOB is 10% of the drill collars weight, PDC bit, (Case 1)

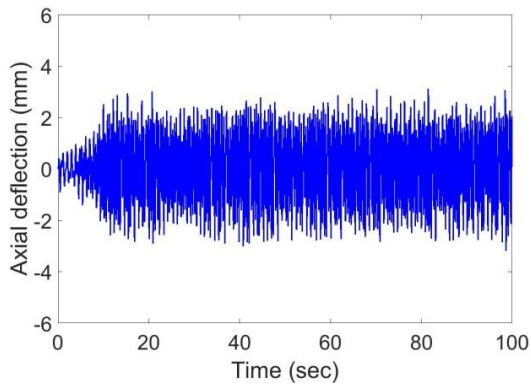


Figure 7. Axial deflection at 200 m above the bit, WOB is 10% of the drill collars weight, PDC bit, (Case 2)

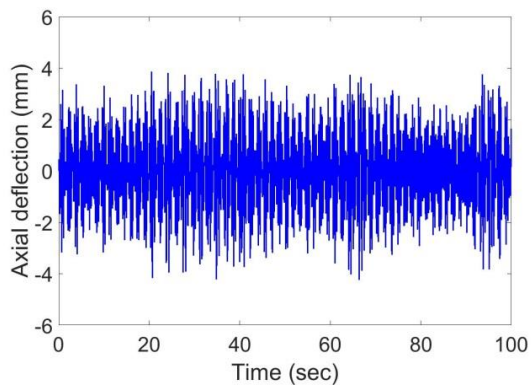


Figure 8. Axial deflection at 200 m above the bit, WOB is 10% of the drill collars weight, RC bit, (Case 1)

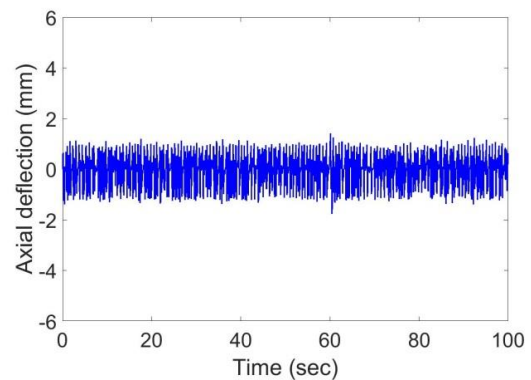


Figure 9. Axial deflection at 200 m above the bit, WOB is 10% of the drill collars weight, RC bit, (Case 2)

As displayed in Figures 8 and 9, Case 2 shows the denser axial vibrations with less amplitudes at a point above the bit. Also, the comparison between these figures with Figures 6 and 7 show that using RC bit intensify the density of axial vibrations.

Figures 10 and 11 show the axial deflections when WOB is 30% of the drill collars weight for PDC bits in cases 1 and 2, respectively.

As shown in Figures 10 and 11, the increase of WOB leads to more axial vibrations. Although due to capturing the response of a point that located in thick part of drill string, this result is not remarkable.

The axial deflections, when WOB is 30% of the drill collars weight for RC bits in cases 1 and 2 are displayed in Figures 12 and 13, respectively.

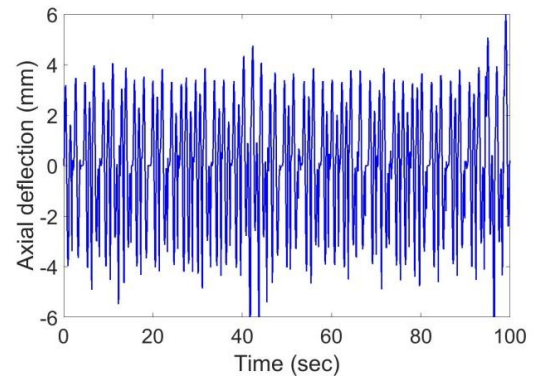


Figure 10. Axial deflection at 200 m above the bit, WOB is 30% of the drill collars weight, PDC bit, (Case 1)

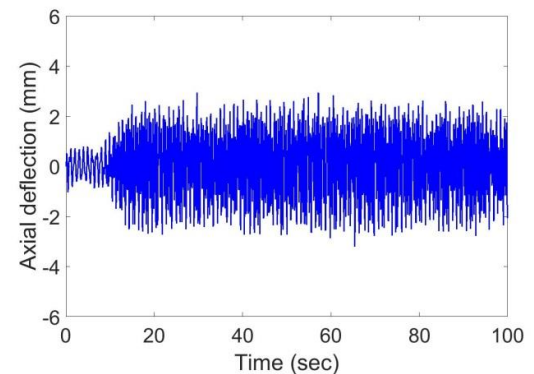


Figure 11. Axial deflection at 200 m above the bit, WOB is 30% of the drill collars weight, PDC bit, (Case 2)

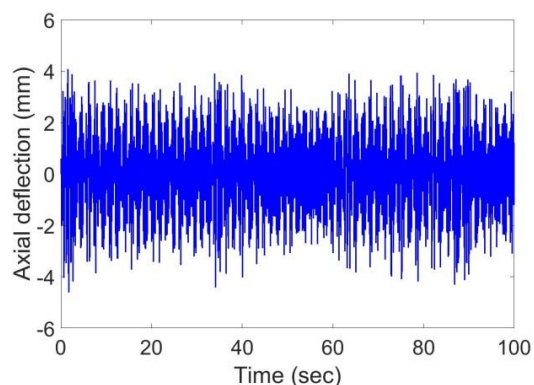


Figure 12. Axial deflection at 200 m above the bit, WOB is 30% of the drill collars weight, RC bit, (Case 1)

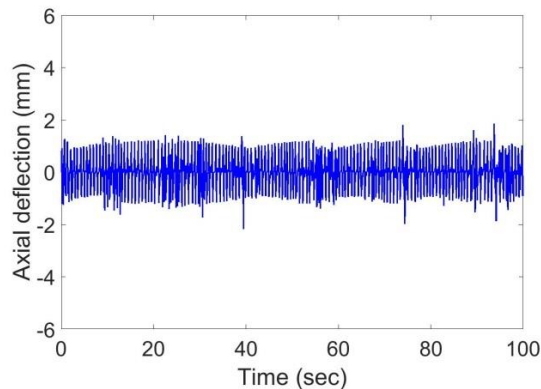


Figure 13. Axial deflection at 200 m above the bit, WOB is 30% of the drill collars weight, RC bit, (Case 2).

As shown in Figures 12 and 13, when the RC bits are used, the axial responses in a point above the bit are denser than PDC bits.

4. CONCLUSION

In this study, the fully coupled non-linear axial vibrations of composite drill strings due to the interaction of two common bits namely; Roller-Cone (RC) bits and Polycrystalline Diamond Compact (PDC) with rock, considering the drill string-wellbore contact, the different weight on bit (WOB) and the different composite configurations were investigated. The gyroscopic effect, and especially the geometric stiffening effect, the axial-torsional-lateral coupling of vibrations and the major non-linear terms have been taken into account. The full-order non-linear equations of the whole length of drill string including drill pipes and drill collars were derived by the finite element method and the Lagrangian approach.

This study proved that the different configurations of composite drill strings showed specific dynamic behavior in different conditions; therefore, composite drill string can be designed for particular purposes. Also, the results imply the remarkable effects of weight on bit and type of bits on the axial vibrations of composite drill strings.

As discussed, when the ply angle decreases, due to increase of axial stiffness, firstly; the maximum amplitudes of responses decrease; secondly, the capability of drill string to transmit the axial vibrations increases, and the drill string become more sensitive to excitations, so the drill string experience the denser axial vibrations at the point above the bit. Also, using RC bit intensifies the density of axial vibrations and the increase of weight on bit leads to more axial vibrations.

5. REFERENCES

1. Finnie, I. and Bailey, J.J., "An experimental study of drillstring vibration", *Journal of Engineering for Industry*, ASME Transaction Vol. 82, No. 2, (1960), 129-135, doi: 10.1115/1.3663020.
2. Bailey, J.J. and Finnie, I., "An analytical study of drillstring vibration", *Journal of Engineering for Industry*, ASME Transaction Vol. 82, No. 2, (1960), 122-128, doi: 10.1115/1.3663017.
3. Wolf, S.F., Zacksenhouse, M. and Arian, A., "Field measurements of downhole drillstring vibrations", Proceedings of the Annual Technical Conference & Exhibition, Las Vegas, (1985), 32-42, doi: 10.2118/14330-MS.
4. Yigit, A.S. and Christoforou, A.P., "Coupled axial and transverse vibrations of oilwell drillstrings", *Journal of Sound and Vibration*, Vol. 195, No. 4, (1996), 617-627, doi: 10.1006/jsvi.1996.0450.
5. Wu, X., Paez, L.C., Partin, U.T. and Agnihotri, M., "Decoupling stick-slip and whirl to achieve breakthrough in drilling performance", Proceedings of the IADC/SPE Drilling Conference and Exhibition, Society of Petroleum Engineers (2010), doi: 10.2118/128767-MS.
6. Bailey J.R. and Remmert, S.M., "Managing drilling vibrations through BHA design optimization", *Drilling and Completion*, Vol. 25, No. 40, (2010), 458-471, doi: 10.2118/139426-PA.
7. Dvoynikov, M., Syzrant sev, V. and Syzrant sevab, K., "Designing a high resistant, high-torque downhole drilling motor", *International Journal of Engineering, Transactions A: Basics*, Vol. 30, No. 10, (2017), 1615-1621, doi: 10.5829/ije.2017.30.10a.24.
8. Wang, H., Guan, Z.C., Shi, Y.C., Liu, Y.W. and Liang D.Y., "Drilling Trajectory Prediction Model for Push-the bit Rotary Steerable Bottom Hole Assembly", *International Journal of Engineering, Transactions B: Applications*, Vol. 30, No. 11, (2017), 1800-1806, doi: 10.5829/ije.2017.30.11b.23.
9. Elsayed, M.A., Dareing, D.W. and Dupuy, C.A. "Effect of downhole assembly and polycrystalline diamond compact (PDC) bit geometry on stability of drillstrings", *Journal of Energy Resources Technology*, Vol. 119, (1997), 159-163, doi: 10.1115/1.2794984.
10. Jansen, J.D., "Nonlinear rotor dynamics as applied to oilwell drillstring vibrations", *Journal of Sound and Vibration*, Vol. 147 No. 1, (1991), 115-135, doi: 10.1016/0022-460X(91)90687-F.
11. Jogi, P.N., Macpherson, J.D. and Neubert, M., "Field verification of model-derived natural frequencies of a drill string", *Journal of Energy Resources Technology*, Vol. 124, No. 3, (2002), 154-162, doi: 10.1115/1.1486018.
12. Spanos, P.D., Chevallier, A.M. and Politis, N.P., "Nonlinear stochastic drill-string vibrations", *Journal of Applied Mechanics*, ASME Transactions, Vol. 124, (2002), 512-518, doi: 10.1115/1.1502669.
13. Khulief, Y.A. and Al-Naser, H., "Finite element dynamic analysis of drillstrings", *Finite Element in Analysis and Design* Vol. 41, (2005), 1270-1288, doi: 10.1016/j.finel.2005.02.003.
14. Ghasemloonia, A., Rideout, D.G. and Butt, S.D., "Analysis of multi-mode nonlinear coupled axial-transverse drillstring vibration in vibration assisted rotary drilling", *Journal of Petroleum Science and Engineering*, Vol. 116, (2014), 36-49, doi: 10.1016/j.petrol.2014.02.014.
15. Trang, G.T.T., Linh, N.H., Linh, N.T.T. and Kien, P.H., "The study of dynamics heterogeneity in SiO₂ liquid", *High Tech and Innovation Journal*, Vol. 1, No. 1, (2020), 1-7, doi: 10.28991/HIJ-2020-01-01-01.

16. Fazelabdolabadi, B. and Golestan, M.H. "Towards bayesian quantification of permeability in micro-scale porous structures – The database of micro networks", *High Tech and Innovation Journal*, Vol. 1, No. 4, (2020), 148-160, doi: 10.28991/HIJ-2020-01-04-02.
17. Battistelli, D., Ferreira, D.P., Costa, S., Santulli C. and Fanguero, R. "Conductive thermoplastic starch (TPS) composite filled with waste iron filings", *Emerging Science Journal*, Vol. 4, No. 3, (2020), 136-147, doi: 10.28991/esj-2020-01218.
18. Furch, J., Nguyen, Q.H. "Lifetime test of tracked vehicle torsion bars using Monte Carlo method", *Emerging Science Journal*, Vol. 4, No. 5, (2020), 376-389, doi: 10.28991/esj-2020-01238.
19. Ha, K., "Innovative blade trailing edge flap design concept using flexible torsion bar and worm drive", *High Tech and Innovation Journal*, Vol. 1, No. 3, (2020), 101-106, doi: 10.28991/HIJ-2020-01-03-01.
20. J.C. Leslie, J.T. Heard, L. Truong, "Advances in composite drilling components lead to evaluation for critical E&P applications", *Advanced Composite Products and Technology*, (2007).
21. Dong, G. and Chen, P. "A review of the evaluation, control, and application technologies for drill string vibrations and shocks in oil and gas well", *Shock and Vibration*, (2016), Article ID 7418635, doi: 10.1155/2016/7418635.
22. Mohammadzadeh, M., Shahgholi, M., Arbabtafti, M. and Yang, J., "Vibration analysis of the fully coupled nonlinear finite element model of composite drill strings", *Archive of Applied Mechanics*, Vol. 90, (2020), 1373-1398, doi: 10.1007/s00419-020-01673-8.
23. Bazoune, A., Khulief, Y.A. and Stephen, N.G., "Shape functions of three-dimensional Timoshenko beam element", *Journal of Sound and Vibration*, Vol. 259, No. 2, (2003), 473-480, doi: 10.1006/jsvi.2002.5122.
24. Su, Y.Y. and Gao, K.L., "Analytical model for adhesively bonded composite panel-flange joints based on the Timoshenko beam theory", *Composite Structures*, Vol. 107, (2014), 112-118, doi: 10.1016/j.compstruct.2013.07.018.
25. Khalkhali, A., Narimanzadeh, N., Khakshournia, S. and Amiri, S., "Optimal design of sandwich panels using multi-objective genetic algorithm and finite element method", *International Journal of Engineering-Transactions C: Aspects*, Vol. 27, No.3, (2013), 395-402, doi: 10.5829/idosi.ije.2014.27.03c.06.
26. Jones, R.M., "Mechanics of Composite Materials", 2nd Ed, Taylor & Francis Inc. (1999).
27. Likens, P., Barbera, F. and Baddeley, V., "Mathematical modeling of spinning elastic bodies for modal analysis", *Journal of American Institute of Aeronautics and Astronautics*, Vol. 11, No. 9, (1973), 1251-1258, doi: doi.org/10.2514/3.6906.

Persian Abstract

چکیده

رشته حفاری به عنوان یک تجهیز استراتژیک در صنایع نفت و گاز شناخته شده و همواره مورد توجه مراکز تحقیقاتی و صنایع بوده است. همراه با توسعه علم کامپوزیت و مزایای فراوان آنها، تکنولوژی رشته حفاری کامپوزیت به سرعت در حال توسعه می باشد. هدف از این تحقیق تحلیل ارتعاشات کوپل شده غیر خطی محوری رشته حفاری کامپوزیت با در نظر گرفتن تماس رشته حفاری - دیواره چاه و بخصوص تماس مته حفاری - سازه کف چاه می باشد. دو نوع متداول مته حفاری با عنوان مته سه کاجه (RC) و مته الماسه (PDC) در نظر گرفته شده اند. رشته حفاری کامپوزیت متشکل از لایه های اورتوتروپ در نظر گرفته شده و برای بدست آوردن نتایج، معادلات دینامیکی غیر خطی مرتبه کامل حاکم بر تمام طول رشته حفاری کامپوزیت عمودی با استفاده از روش انرژی و معادلات لاگرانژ و به کمک روش المان محدود استخراج و حل می گردند. کوپل انواع ارتعاشات محوری - جانبی - پیچشی در معادلات غیر خطی، اثر ژيروسکوپی، ترمهای غیر خطی اصلی و اثر سختی هندسی ناشی از تقابل مته و نیروی وزن رشته حفاری در نظر گرفته شده اند. ارتعاشات کوپل شده غیر خطی محوری رشته حفاری کامپوزیت ناشی از تقابل دو نوع مته حفاری و سازه کف چاه، با در نظر گرفتن وزن روی مته (WOB) متفاوت برای دو رشته حفاری با ساختار کامپوزیتی متفاوت، که توانایی نشان دادن روند کلی تغییرات را دارند، مورد مطالعه قرار گرفته است.
